Acta Neuropathologica (2020) 140:359–375
https://doi.org/10.1007/s00401-020-02189-9

ORIGINAL PAPER

Lesion stage-dependent causes for impaired remyelination in MS

Katharina Heß[1] · Laura Starost[1,2] · Nicholas W. Kieran[3] · Christian Thomas[1] · Maria C. J. Vincenten[6] · Jack Antel[3] · Gianvito Martino[4,5] · Inge Huitinga[6] · Luke Healy[3] · Tanja Kuhlmann[1]

Received: 31 March 2020 / Revised: 16 June 2020 / Accepted: 28 June 2020 / Published online: 24 July 2020

Abstract

Multiple sclerosis (MS) is the most frequent demyelinating disease and a leading cause for disability in young adults. Despite significant advances in immunotherapies in recent years, disease progression still cannot be prevented. Remyelination, meaning the formation of new myelin sheaths after a demyelinating event, can fail in MS lesions. Impaired differentiation of progenitor cells into myelinating oligodendrocytes may contribute to remyelination failure and, therefore, the development of pharmacological approaches which promote oligodendroglial differentiation and by that remyelination, represents a promising new treatment approach. However, this generally accepted concept has been challenged recently. To further understand mechanisms contributing to remyelination failure in MS, we combined detailed histological analyses assessing oligodendroglial cell numbers, presence of remyelination as well as the inflammatory environment in different MS lesion types in white matter with in vitro experiments using induced-pluripotent stem cell (iPSC)-derived oligodendrocytes (hiOL) and supernatants from polarized human microglia. Our findings suggest that there are multiple reasons for remyelination failure in MS which are dependent on lesion stage. These include lack of myelin sheath formation despite the presence of mature oligodendrocytes in a subset of active lesions as well as oligodendroglial loss and a hostile tissue environment in mixed active/inactive lesions. Therefore, we conclude that better in vivo and in vitro models which mimic the pathological hallmarks of the different MS lesion types are required for the successful development of remyelination promoting drugs.

Keywords Multiple sclerosis · Remyelination · Oligodendrocytes · Microglia

Introduction

Multiple sclerosis (MS) is the most frequent inflammatory and demyelinating disease of the CNS; it affects approximately 2.3 million people worldwide [15]. Approximately 50% of the patients require a walking aid after 10–15 years of disease duration. The socioeconomic costs are significant; in 2013, the annual costs for MS in the US have been estimated to be approximately 10 billion $ per year [1]. Histopathologically, MS is characterized by multifocal demyelinating lesions, inflammatory infiltrates (macrophages, T cells, and B cells), damaged and reduced numbers of axons, and loss of oligodendrocytes [45]. Based on density and distribution of blood-derived monocytes and CNS-resident microglia (subsequently summarized as myeloid cells) active, mixed active/inactive and inactive lesions can be distinguished as described in an updated histological classification of MS [38].

Demyelinated axons are either remyelinated or remain chronically demyelinated making them especially vulnerable

Electronic supplementary material The online version of this article (https://doi.org/10.1007/s00401-020-02189-9) contains supplementary material, which is available to authorized users.

✉ Tanja Kuhlmann
tanja.kuhlmann@ukmuenster.de

1 Institut für Neuropathologie, Universitätsklinikum Münster, Pottkamp 2, 48149 Münster, Germany

2 Max Planck Institut für Molekulare Biomedizin, 48149 Münster, Germany

3 Montreal Neurological Institute, McGill University, Montreal, Canada

4 Neuroimmunology Unit, Division of Neuroscience, Institute of Experimental Neurology, IRCCS San Raffaele Hospital, 20132 Milan, Italy

5 Vita Salute San Raffaele University, 20132 Milan, Italy

6 Department of Neuroimmunology, The Netherlands Institute for Neuroscience, Amsterdam, The Netherlands

to injury mediated by the immune system or lack of trophic support [25]. Axonal injury and loss are already present in early MS lesion stages and are the underlying cause for disease progression [37, 63, 65]. The formation of new myelin sheaths around axons after a demyelinating event, termed remyelination, represents an endogenous repair process which restores the conduction of action potentials, provides trophic support to axons, and protects against axonal damage [18, 33, 47]. Also, recent histological and imaging studies suggest that remyelination contributes to clinical recovery [5, 46]. In different lesions from the same patient, extent of remyelination can vary significantly [56, 57] and lesion localization may influence the extent of remyelination [2, 29, 57].

In animal experiments, proliferation and migration of oligodendrocyte precursor cells (OPC) as well as their differentiation into mature myelinating oligodendrocytes is required for successful remyelination. These complex processes are regulated by the interaction of OPC and oligodendrocytes with neurons and axons, astrocytes as well as immune cells, such as macrophages/microglia, T cells, and B cells (for review see [24, 25, 27, 42]). In progressive MS, OPC are still present in MS lesions albeit in reduced numbers and unevenly distributed, whereas mature oligodendrocytes are almost completely lacking [11, 39, 69]. These findings resulted in the concept of impaired oligodendroglial differentiation as contributing factor for limited remyelination in chronic MS [25, 62]. In animal studies, several signalling cascades have been identified, inhibiting the differentiation of OPC into mature myelinating oligodendrocytes which may be activated by inflammatory cells present in MS lesions. In contrast, myeloid cells polarized into an M2 (anti-inflammatory) phenotype promote oligodendroglial differentiation in experimental animal studies [52]. Extensive research and drug development efforts have been undertaken to identify drugs which promote oligodendroglial differentiation and by that remyelination [16, 50, 51, 53]. Among the identified drugs were anti-Lingo-1 antibodies and clemastine which were tested in clinical phase II trials [8, 9, 30]. Both compounds successfully promoted remyelination in several demyelinating animal models; however, they had a very modest effect in clinical phase II trials [8, 9, 30].

The view that differentiation of OPC into mature myelinating oligodendrocytes is required for successful remyelination in humans has been challenged recently. Measuring the integration of ^{14}C derived from nuclear testing into DNA of oligodendroglial lineage cells Yeung et al. suggest that pre-existing oligodendrocytes and not proliferating OPC may contribute to remyelination in MS [71]. Moreover, Jäkel et al. performed scRNA-seq analysis and identified different subpopulations of OPC and oligodendrocytes in brain tissue samples from MS patients and healthy individuals which only partly overlapped with oligodendroglial subsets identified in mouse brains [34, 48]. They propose that the loss of certain subpopulations and the skewing of the differentiation program to other subclasses of mature oligodendrocytes contribute to impaired remyelination in MS [34].

Here, we demonstrate that in active/demyelinating white matter lesions, mature oligodendrocytes are preserved and that a subset of these lesions displays marked remyelination. In mixed and inactive lesions, oligodendroglial loss is most pronounced in the lesion center suggesting that extended time periods of demyelination contribute to oligodendroglial cell death. Mixed lesions are almost completely lacking remyelination and this lack of remyelination is associated with a relative increase in TMEM119$^+$ microglia and iNOS$^+$ myeloid cells. Moreover, in vitro experiments demonstrate that supernatants from M1 (pro-inflammatory) polarized primary human microglia, but not M2 or M0 (unstimulated) polarized microglia impair the terminal differentiation of hiOL into myelin basic protein (MBP) positive mature oligodendrocytes.

In summary, our data suggest that there are multiple reasons for remyelination failure in MS depending on lesion stage. Our findings indicate that in active/demyelinating lesions, impaired myelin sheath formation despite the presence of mature oligodendrocytes contributes to remyelination failure, whereas in mixed lesions, loss of oligodendrocytes and a hostile tissue environment prevent successful remyelination. Therefore, for the development of remyelination promoting drugs, new animal models are required which better mimic the different MS lesion stages. Furthermore, drug development efforts promoting remyelination should not only target oligodendroglial differentiation but also other important steps required for successful remyelination, such as proliferation and migration of OPC, myelin sheath formation by mature oligodendrocytes, prevention of oligodendroglial loss as well as modulation of the inflammatory environment.

Materials and methods

Materials

The study was performed retrospectively on a collection of paraffin-embedded brain biopsy and autopsy tissue specimens from 62 patients. The cohort comprised 38 biopsy tissue samples from 32 patients and 113 MS lesions (81 tissue blocks) from autopsies from 30 patients. Among the autopsies, 53 tissue blocks with 71 lesions from 17 patients were derived from the autopsy collection of the Institute of Neuropathology, University Hospital Münster. From The Netherlands Brain Bank, Netherlands Institute for Neuroscience, Amsterdam (open access: https://www.brainbank.nl), 28 tissue blocks with 42 lesions from 13 patients were obtained;

all material has been collected from donors for or from whom a written informed consent for a brain autopsy and the use of the material and clinical information for research purposes had been obtained by the NBB. Brain biopsies were performed as part of diagnostic evaluation of unclear monofocal lesions that showed atypical MRI findings. None of the study authors were involved in decision-making with respect to biopsy or autopsy. The study was approved by the Ethics Committee of the University of Münster and McGill University (Az: 2016-026-f-S, 2016-165-f-S, 2012-407-f-S, 2011-023-f-S, ANTJ 1988-3). Clinical details are provided in Table 1.

Criteria for determination of lesion activity

All lesions included in our study were located within the white matter of the brain and fulfilled the generally accepted histological criteria for the diagnosis of MS [38]. The lesion

Table 1 Clinical details

Total number of patients	62
Biopsies	
Total number of tissue samples	38
Male:female patients	9:23
Median age ± SD	49 ± 14.49 years
Lesion type: activity	
Active/demyelinating	36 94.73% of biopsies
Active/post-demyelinating	2 5.26% of biopsies
Median number of tissue samples analyzed for each individual ± SD (1 tissue sample: 29 patients; 2 tissue samples: 2 patients and 5 tissue samples: 1 patient)	1 ± 0.7
Autopsies	
Total number of lesions	113
Male:female patients	12:18
Median age ± SD	59 ± 14.28 years
Median disease duration ± SD (disease duration unknown for 12 patients)	24 ± 13.58 years
Median postmortem delay ± SD (postmortem delay unknown for 17 patients)	8 h 25 min ± 1 h 47 min
Disease course and number of patients	
RRMS	2
SPMS	16
PPMS	2
Unknown	10
Cause of death	
Cardiovascular failure	6
Respiratory failure/pneumonia	9
Sepsis	3
Euthanasia	3
Other	2
Unknown	7
Lesion type: activity	
Active/post-demyelinating	15 13.27% of autopsies
Mixed	35 30.97% of autopsies
Inactive	63 55.75% of autopsies
Median number of lesions analyzed for each individual ± SD (1 lesion: 5 patients; 2 lesions: 7 patients; 3 lesions: 3 patients; 4 lesions: 7 patients; 5 lesions: 3 patients; 6 lesions: 3 patients; 10 lesions: 1 patient; 14 lesions: 1 patient)	3.5 ± 2.74

NA not applicable, *RRMS* relapsing remitting MS, *SPMS* secondary progressive MS, *PPMS* primary progressive MS, *NAWM* normal appearing white matter

classification is based on the updated histological classification of MS lesions by Kuhlmann et al. using immunohistochemistry (IHC) for MBP to detect demyelination and CD68 to determine number and distribution of myeloid cells (comprising blood-derived monocytes and CNS-resident microglia) [38]. Active lesions were hypercellular and characterized by a diffuse infiltration of the complete lesion area with numerous $CD68^+$ myeloid cells. The density of these cells was higher than in the surrounding periplaque white matter (PPWM) (directly adjacent to the lesions) and normal appearing white matter (NAWM) (further away from the lesions). In biopsy lesions, NAWM and PPWM were summarized as non-demyelinated white matter (NDWM), since biopsy specimens were frequently fragmented and distance between lesion and non-demyelinated white matter was not always unambiguous. Active lesions were further subdivided into active/demyelinating as well as active/post-demyelinating lesions. In active/demyelinating lesions, numerous myeloid cells containing MBP^+ myelin degradation products in their cytoplasm were observed, whereas myeloid cells in active/post-demyelinating lesions lacked these myelin breakdown products. Mixed active/inactive lesions (formerly called chronic active lesions, including so called smoldering and slowly expanding lesions) were characterized by a hypocellular lesion center and a rim of activated myeloid cells at the border of the lesion, whereas the lesion center was almost completely depleted of myeloid cells. For simplicity, mixed active/inactive lesions will be subsequently termed mixed lesions. Inactive lesions were hypocellular within the whole lesion area with only few myeloid cells present. The density of myeloid cells in inactive lesions was reduced in comparison to that in NDWM.

Criteria for semiquantitative analysis of remyelination

In biopsies and autopsies, the extent of remyelination was assessed in all lesions using a semiquantitative score. In biopsies, remyelination was identified as thin, irregular formed myelin sheaths utilizing IHC for MBP. Because biopsy samples frequently display only parts of the lesion, we quantified the extent of remyelination using the following categories: 0 = complete absence of remyelination, 1 = individual oligodendrocytes extending remyelinating processes, 2 = patchy remyelination, 3 = remyelination throughout the sampled lesion area [29].

In autopsy cases, regions of remyelination were identified by thin myelin sheaths by IHC for MBP and pale staining in Luxol fast blue (LFB)–periodic acid Schiff (PAS) staining. In the majority of autopsy cases, complete lesions were sampled. Therefore, the lesions were classified depending on the percentage of lesion area that was remyelinated: 0 = no remyelination or presence only at the lesion border making up less than 10% of the whole lesion area, 1 = remyelination was found in more than 10, but less than 50% of the whole lesion area, 2 = more than 50% of the lesion remyelinated, 3 = completely remyelinated lesion.

Immunohistochemistry

For IHC, tissue specimens were fixed in 4% paraformaldehyde (PFA) and embedded in paraffin. Biopsy and autopsy tissues were cut in 4-µm-thick sections that were stained with hematoxylin and eosin and LFB-PAS. Immunohistochemical stainings were performed using the Dako REAL^{TM} Detection System (#K5001, Dako) and an automated immunostainer (AutostainerLink 48, Dako). IHC was performed using a biotin–streptavidin technique. In short, sections were deparaffinized and intrinsic peroxidase activity was blocked by incubation with 5% H_2O_2 in phosphate-buffered saline (PBS) for 5 min afterwards. Primary antibodies were applied as listed in Supplementary Table 1, online resource. IHC was completed using species-specific biotinylated secondary anti-mouse, rat, or rabbit antibodies followed by incubation with streptavidin/peroxidase complex and the reaction product was developed with diaminobenzidine. For myelin stainings, staining quality was evaluated using vessels or grey matter structures as internal controls. Stained sections that did not show a positive staining signal for e.g. NOGOA or OLIG2 in the normal appearing white or grey matter were excluded from further analyses. Therefore, and due to limited tissue material of some biopsies, number of analyzed lesions varies between different quantifications. For quantitative evaluation, sections of interest stained by IHC were analyzed at 100-fold magnification using a morphometric grid. For quantifications of small lesions, the whole lesion area was analyzed and for quantifications of more extensive lesions, at least ten visual fields per region (e.g. lesion center, lesion border, PPWM etc.) were analyzed. For each region of interest, average counts per square millimeter were calculated and compared by statistical analysis. In autopsy lesions, we analyzed different lesion areas. The edge between the lesion itself and NDWM could be identified in all stainings due to different tissue structure in the lesion. Lesion border was defined as the visual fields directly adjacent to the edge inside the lesion at 100-fold magnification. PPWM was defined as the visual fields directly adjacent to the edge outside the lesion at 100-fold magnification. NAWM was characterized as further away from the lesion, at least five visual fields at 100-fold magnification distant from PPWM. As center, we defined the region furthest away from all lesion borders. The region of interest termed "between center and border" was defined as halfway between lesion border and lesion center (see also Fig. 2a). The ratio (eg. ratio of $TMEM119^+/CD68^+$ cells) was determined by

staining and quantifying the numbers of positive cells for the individual markers on consecutive sections.

For double IHC, primary antibodies derived from different species were used. Sections were deparaffinized and blocked in 10% PBS/10% fetal calf serum (FCS) for 20 min. Afterwards, tissues were incubated with the primary antibodies overnight at 4 °C. After three washing steps with PBS, Alexa Fluor 488 and Cy3 coupled secondary antibodies (1:250, Jackson ImmunoResearch Laboratories) were applied for 1 h at room temperature. DAPI was added in the second washing steps to counterstain the nuclei using Roti Mount FluorCare DAPI (Dako).

Generation of induced pluripotent stem cell-derived oligodendrocytes

iPSC were kindly provided by Prof. Gianvito Martino, San Raffaele Hospital Milan (ethic approval from Banca INSpe). hiOL were generated as described previously [22]. In short, $1.5*10^5$ iPSC-derived neural progenitor cells (NPC) were differentiated as described [60] and seeded onto one well of a matrigel (corning)-coated 12-well plate in NPC medium consisting of equal parts of neurobasal (Invitrogen) and DMEM-F12 medium (Invitrogen) with 1:100 B27 supplement lacking vitamin A (Invitrogen), 1:200 N2 supplement (Invitrogen), 1% penicillin/streptomycin/glutamine (PSG), 150 µM ascorbic acid (AA), 3 µM CHIR99021 (Axon Medchem) and 0.5 µM SAG (Cayman Chemical). The next day, cells were lentivirally transduced with a polycistronic lentiviral vector containing the coding regions of human SOX10, OLIG2, and NKX6.2 followed by an IRES-pac cassette allowing puromycin selection for 16 h. The following day, cells were washed and allowed to recover in NPC medium for 1 day. Subsequently, medium was replaced by glial induction medium (GIM) consisting of DMEM-F12 with 1:100 B27 supplement lacking vitamin A, 1:200 N2 supplement, 1% PSG, 1 µM SAG, 10 ng/mL NT3 (Peprotech), 10 ng/mL PDGF-AA (Peprotech), 10 ng/mL IGF-I (Peprotech), 100 µM AA (Sigma), 1:1000 Trace Elements B (Corning), 15 ng/mL T3 (Sigma) and 1 ng/mL bFGF-2 (Peprotech). After 4 days, GDM consisting of DMEM-F12 with 1:100 B27 supplement lacking vitamin A, 1:200 N2 supplement, 1% PSG, 10 ng/mL NT3, 50 µM dbCAMP (Sigma), 10 ng/mL IGF-I, 100 µM AA, 1:1000 Trace Elements B and 60 ng/mL T3 was applied to the cells. Medium was changed every other day. From day 3 to day 8 of differentiation, 0.75 µg/mL puromycin was applied to remove non-transduced cells.

Supernatants of primary microglia and respective media controls were applied from day 4 to day 21 of differentiation to assess early differentiation. To elucidate effects on proliferation, terminal differentiation and cell death untreated hiOL were sorted for O4 at day 21 of differentiation and subsequently treated with supernatants of primary microglia and media controls until day 35 of differentiation.

Flow cytometry of hiOL

hiOL were sorted and quantified for O4 by utilizing anti-O4-APC antibody according to manufacturer's instructions (Miltenyi). Briefly, hiOL were detached by accutase. Next, cells were washed, filtered through a 40 µm filter and cell numbers were determined. Subsequently, 2 µL of anti-O4-APC antibody per $1*10^6$ cells were applied and incubated for 10 min at 4 °C in the refrigerator. Afterwards, cells were washed and analyzed and sorted using a FACSAria IIu cell sorter (BD Biosciences). $O4^+$ hiOL, identified using unstained cells and isotype controls, were immediately seeded in GDM and used for further experiments analyzing the effects of microglia supernatants. Gating strategy for $O4^+$ cells was described previously [67]. Sorted hiOL contain less than 1% GFAP positive cells (data not shown).

Immunocytochemistry

For immunocytochemistry (ICC), cells were fixed in 4% PFA. After three washing steps, blocking buffer consisting of 5% normal goat serum/5% FCS in PBS was applied for 30 min. Next, anti-O4 antibody (R&D Systems) was applied in a dilution of 1:1000 in blocking buffer and incubated at 4 °C overnight. The next day, cells were washed three times and Alexa Fluor-conjugated secondary antibody was applied for 1 h at RT. After three additional washing steps, 0.1% triton was applied to permeabilize the cells for 10 min followed by additional three washing steps. Next, anti-MBP (abcam), anti-Ki-67 (abcam) or anti-cleaved caspase 3 (R&D Systems) antibodies were applied in blocking buffer and cells were incubated for 1 h at RT. For antibody dilutions see Supplementary Table 1, online resource. After three washing steps, Alexa Fluor-conjugated secondary antibody was applied for 1 h at RT. Cells were again washed three times and subsequently visualized on a Leica DMI6000 B inverted microscope. DAPI was used to counterstain the nuclei.

Generation of supernatants of primary microglia

Primary human microglia were isolated from fetal and adult tissue samples, followed by standard culturing and activation techniques as previously described [20]. Briefly, adult microglia were derived from surgically resected brain tissue, removed for the treatment of nonmalignant temporal lobe epilepsy. The tissue provided was outside of the suspected focal site of epilepsy pathology, histopathological changes were excluded by an experienced neuropathologist, and histologically healthy specimens were included. Tissue was obtained in pieces < 1 mm^3 and treated with DNase

(Roche) and trypsin (Thermo Fisher) for 30 min at 37 °C. Following dissociation through a nylon mesh (37 µm), the cell suspension was separated on a 30% Percoll gradient (GE Healthcare) at 31,000 × g for 30 min. Glial cells (oligodendrocytes and microglia) were collected from underneath the myelin layer, washed, and plated. Microglia were separated by the differential adhesion properties of the cells and plated in minimum essential medium (MEM; Sigma-Aldrich) supplemented with 5% FBS (Wisent), 0.1% penicillin/streptomycin (Thermo Fisher), and 0.1% L-glutamine (Thermo Fisher). Human fetal microglia were isolated from CNS tissue (17–23 weeks of gestation), obtained from the University of Washington Birth defects research laboratory (BDRL, project#5R24HD000836-51). Briefly, brain tissue was minced and treated with DNase/trypsin. Tissue was then dissociated through a nylon mesh and cells were plated in high glucose DMEM supplemented as above. After 10–14 days in culture, floating microglia were harvested and plated in supplemented DMEM. The purity of the cultures was routinely higher than 90% [21, 41].

For M1 stimulation, cells were treated with human granulocyte–macrophage colony-stimulating factor (GM-CSF, 5 ng/mL, PeproTech) for 5 days followed by 1 h stimulation with IFNγ (20 ng/mL, Invitrogen) and 48 h stimulation with lipopolysaccharide (LPS) (serotype 0127:B8, 100 ng/mL, Sigma-Aldrich). For M2 stimulation, cells were treated with macrophage colony-stimulating factor (M-CSF, 25 ng/mL, PeproTech) for 5 days followed by 48 h stimulation with IL-4 (20 ng/mL, Invitrogen) and IL-13 (20 ng/mL, PeproTech). All supernatants were collected 48 h following activation; base media with addition of cytokines, in the absence of cells were used as controls.

RNA isolation and qRT-PCR

RNA isolation and qRT-PCR were performed to confirm the polarization of microglia. Briefly, following collection of supernatants, cells were washed once with warm PBS and lysed in TRIzol reagent (Invitrogen). Total RNA extraction was performed using standard protocols followed by DNAse treatment according to the manufacturer's instructions (Qiagen). For gene expression analysis, random hexaprimers and Moloney murine leukemia virus reverse transcriptase were used to perform standard reverse transcription. Analysis of individual gene expression was conducted using TaqMan probes to assess expression relative to *GAPDH*.

Statistical analysis

All statistics were calculated using the GraphPad Prism 5 software (GraphPad Software). To compare two groups, Student's two-tailed *t* test was applied. For comparison of three or more groups, Bonferroni-corrected one-way ANOVA was performed. All tests were classified as significant if the *p* value was less than 0.05 ($*p < 0.05$, $**p < 0.01$, $***p < 0.001$).

Results

Activity and localization of MS lesions

We analyzed 153 lesions from 62 patients. To classify the lesions we used CD68 and MBP as suggested in the updated histological classification for MS [38]. All biopsy tissue samples were classified as active lesions; among them, 36 as active/demyelinating and 2 as active/post-demyelinating. Among the autopsy tissue samples, we found 15 active (all active/post-demyelinating lesions), 35 mixed, and 63 inactive lesions. In patients from which we had four or more lesions available ($n = 13$, all autopsies), we observed predominantly a mixture of different lesion types. Additionally, three patients displayed only inactive and one patient only active lesions. Of the lesions, 26% were located subcortically, 24% periventricularly, and 9% within the cerebellum. The remaining 41% of the lesions were located in the brain hemispheres, but were neither adjacent to the cortex nor the ventricular system.

Oligodendrocytes are preserved in active/demyelinating lesions, but lost in the center of mixed lesions

We examined the numbers of oligodendrocytes in MS tissue sections using different oligodendroglial markers, such as OLIG2, NOGOA, and tubulin polymerization promoting protein (TPPP/p25) (Fig. 1a–c). OLIG2 labels OPC as well as mature oligodendrocytes, whereas NOGOA and TPPP/p25 are only expressed by mature oligodendrocytes (Fig. 1a, b) [31, 40]. However, our data suggest that NOGOA and TPPP/p25 do not label exactly the same oligodendroglial populations as the absolute numbers of $NOGOA^+$ and $TPPP/p25^+$ cells differ. In a first step, we quantified the number of $TPPP/p25^+$ oligodendroglial lineage cells in NDWM ($n = 117$), active/demyelinating ($n = 24$), active/post-demyelinating ($n = 16$), mixed ($n = 34$) and inactive lesions ($n = 46$). The numbers of $TPPP/p25^+$ oligodendrocytes were significantly reduced in active/post-demyelinating, mixed and inactive lesions, but not in active/demyelinating lesions compared to NDWM (Fig. 1d). To validate TPPP/p25 numbers and further characterize oligodendroglial lineage cell numbers in NDWM as well as active/demyelinating lesions, we quantified the numbers of $OLIG2^+$ and $NOGOA^+$ oligodendrocytes and observed no significant differences (Fig. 1e, f). Similarly,

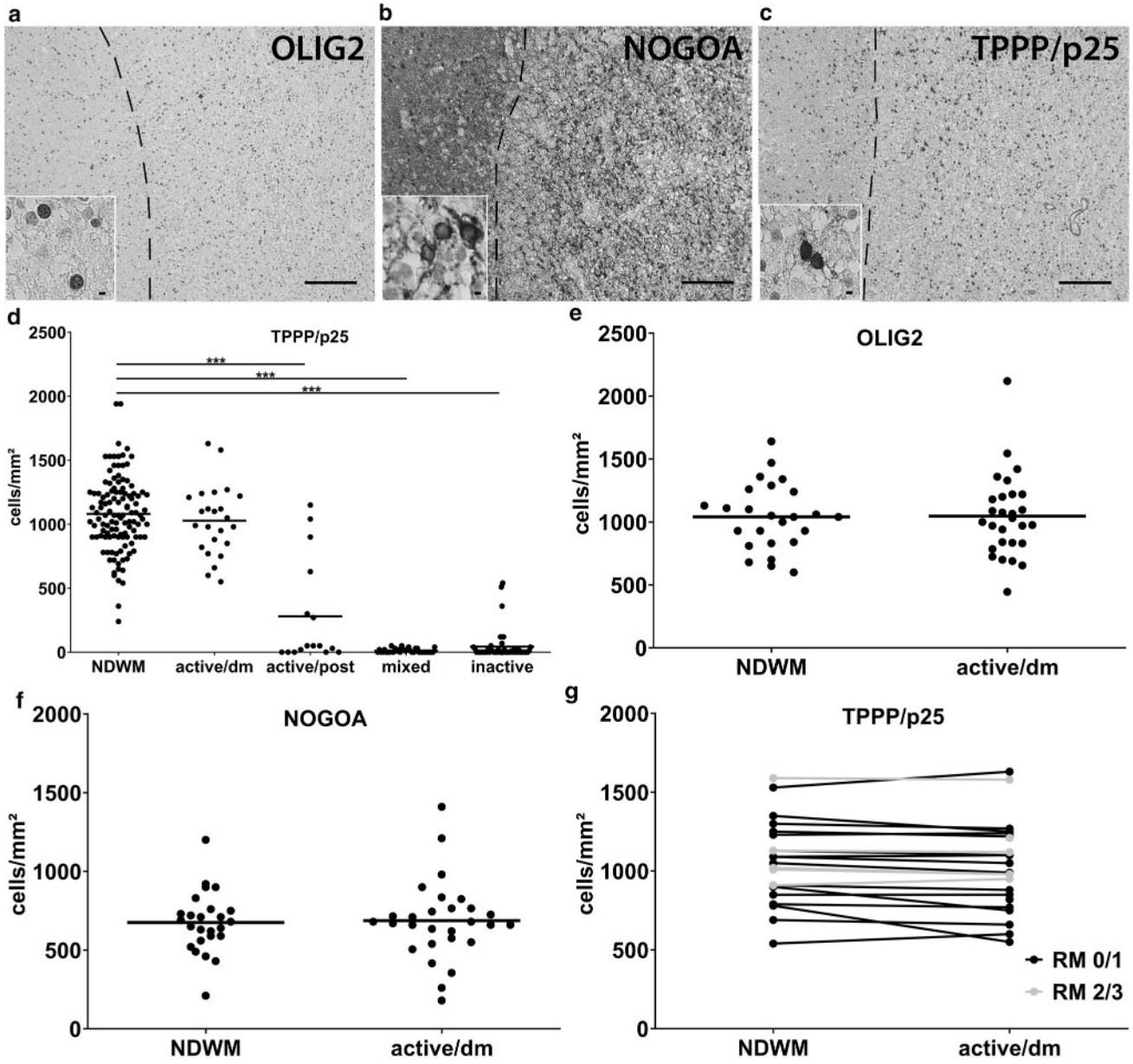

Fig. 1 Preservation of oligodendrocytes in active/demyelinating lesions. **a–c** OLIG2$^+$, NOGOA$^+$ and TPPP/p25$^+$ oligodendrocytes were identified using IHC. Inserts show oligodendrocytes in higher magnification. **d** Quantification of oligodendrocytes in different lesion types and NDWM using TPPP/p25. **e**, **f** Quantification of OLIG2$^+$ and NOGOA$^+$ oligodendrocytes demonstrate comparable cell numbers in active/demyelinating as well as in NDWM. **g** When comparing tissue samples containing NDWM and active/demyelinating lesions, no significant differences in numbers of TPPP/p25$^+$ oligodendrocytes were observed. Lesions with marked remyelination are indicated in blue, lesions with limited remyelination in black. Scale bars in a to c: 200 µm, scale bars in the inserts in a to c 6.25 µm. *OLIG2* oligodendrocyte transcription factor, *TPPP/p25* tubulin polymerization promoting protein, *NDWM* non-demyelinated white matter, *active/dm* active/demyelinating lesions, *active/post* active/post-demyelinating lesions, *mixed* mixed active/inactive lesions, *inactive* inactive lesions, *RM 0/1* remyelination score 0 or 1, *RM 2/3* remyelination score 2 or 3

when comparing individual lesions which contained NDWM and active/demyelinating lesion areas, no marked decrease in the numbers of oligodendrocytes was observed either (Fig. 1g; Supplementary Fig. 1, online resource).

Next, we analyzed oligodendroglial numbers in mixed lesions from which we had the total lesion area available in more detail. In formalin-fixed paraffin-embedded autopsy material, TPPP/p25 labels oligodendroglial lineage cells more reliably than OLIG2 or NOGOA suggesting that the TPPP/p25 epitope is more stable than NOGOA and OLIG2 epitopes identified by the appropriate antibodies. Therefore, we focused on TPPP/p25 to quantify the numbers

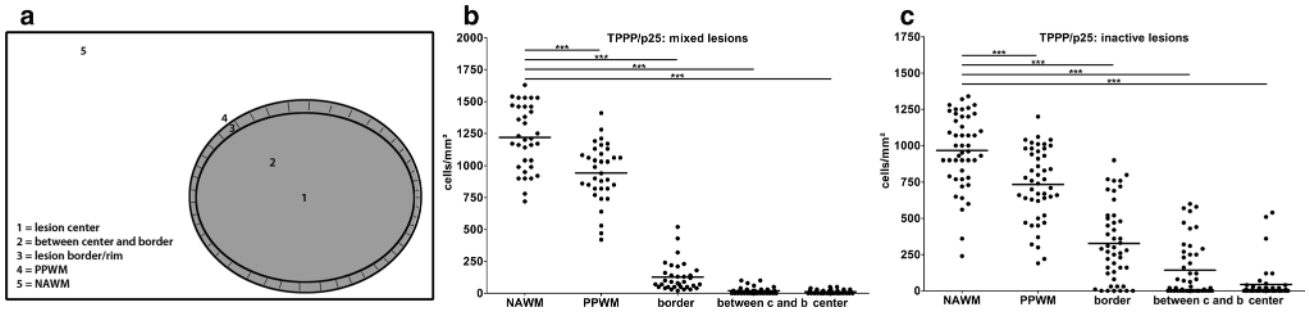

Fig. 2 Loss of oligodendrocytes in mixed and inactive lesions. **a** Schematic drawing indicating the different areas in which oligodendroglial cell numbers were quantified. **b**, **c** Immunohistochemistry for TPPP/p25 revealed continuous decrease in TPPP/p25$^+$ oligodendrocytes from NAWM to the lesion center in mixed and inactive lesions. *TPPP/p25* tubulin polymerization promoting protein, *PPWM* periplaque white matter, *NAWM* normal appearing white matter, *border* lesion border/rim, *between c and b* between center and border of lesion, *center* lesion center

of oligodendrocytes in autopsy material. The numbers of TPPP/p25$^+$ oligodendrocytes in NAWM, PPWM, at the lesion border, between the lesions border and the center as well as in the lesion center were determined (Fig. 2a). In mixed lesions, the border represents the rim which contains myeloid cells. We observed a significant decrease in oligodendroglial numbers in the different lesion areas including the border as well as PPWM compared to NAWM (Fig. 2b). Similar changes in oligodendroglial numbers were also observed in inactive lesions; however, the oligodendroglial loss was more pronounced in the border of mixed compared to inactive lesions (Fig. 2b, c).

These results demonstrate that there is no major loss of oligodendrocytes in active/demyelinating lesions, but a decrease of oligodendroglial numbers in the lesion center in mixed and inactive lesions.

Presence of marked remyelination in a subset of active/demyelinating lesions

Next, we studied the correlation between oligodendrocytes and remyelination in more detail. Results from longitudinal imaging studies suggest that remyelination occurs within the first 5–6 months after initiation of a demyelinating event [6, 13]. Therefore, we focused on active/demyelinating lesions from biopsies ($n=36$), since these are the lesions with the highest probability of ongoing remyelination. To quantify the extent of remyelination, we used a semiquantitative score reaching from 0 (no remyelination) to 3 (complete remyelination of the sampled lesion area) (Fig. 3a, b). In active/demyelinating lesions, 14 out of 36 lesions (=39%) displayed marked remyelination (score 2 or 3) (Fig. 3c). We then compared the numbers of oligodendrocytes in lesions with marked versus limited remyelination (score 0 and 1) (Fig. 3d–f). We observed no significant differences in the numbers of OLIG2$^+$, NOGOA$^+$ and TPPP/p25$^+$ oligodendrocytes in lesions with marked compared to limited remyelination. Additionally, we also compared the ratio of NOGOA$^+$/OLIG2$^+$ oligodendrocytes which is equivalent to the proportion of mature oligodendrocytes in the total oligodendroglial population. No significant difference between lesions with and without marked remyelination was observed (Fig. 3g). Furthermore, we quantified the percentage of actively dividing oligodendrocytes using double IHC for OLIG2 and Ki-67 (Fig. 3h). We focused our analyses on a subset of active/demyelinating lesions with relatively high numbers of proliferating cells identified by IHC for Ki-67 alone ($n=21$). The percentage of actively dividing OLIG2$^+$/Ki-67$^+$ oligodendrocytes was below 2% in all lesions studied and no differences between lesions with and without marked remyelination were detected (Fig. 3h).

In summary, these data suggest that marked remyelination occurs in a subset of active lesions. However, no correlation between oligodendroglial cell numbers, the ratio between mature and total oligodendroglial cell numbers or oligodendroglial proliferation, and the presence of marked remyelination was observed. These results suggest that in lesions with low remyelination scores impaired myelin sheath formation but not reduced oligodendroglial differentiation contributes to lack of remyelination.

Reduced remyelination in mixed lesions

In a next step, we compared the extent of remyelination in active ($n=53$), mixed ($n=35$) and inactive ($n=63$) lesions. In active lesions (active/demyelinating as well as active/post-demyelinating) and inactive lesions, a variable extent of remyelination was observed ranging from lesions completely lacking remyelination (score 0) (Fig. 4a) to completely remyelinated lesions (score 3) (Fig. 4b). However, mixed lesions displayed a more uniform pattern with the vast majority of lesions lacking remyelination (31 out of 35 lesions); while the remaining lesions (4 out of 35) displayed remyelination